

Long-time Scale Color Changes of Flat-spectrum Radio Quasars

Zhou Li, Xu Guangyang, Wang Lisa, Chen Jiufu, Li Xiaopan

College of Physics and Information Engineering Zhaotong University Zhaotong 657000, China

Keywords: Photochromism; Change of color index; Relevance

Abstract: On the basis of introducing the flare variants, flat-spectrum radio quasars and SMARTS projects, this paper briefly analyses the historic light-change curves and color-index-change curves of a typical flat-spectrum radio quasar PKS 2142-75 in each band. The results show that the target's photodynamic activity is intense, and there is not much correlation between color index and brightness. The paper makes a statistical analysis of the long-term color change of the flat-spectrum radio quasar in the SMARTS source. The results show that only a few sources show color changes, which indicates that the light spectrum of the flat-spectrum radio quasar is very complicated.

1. Introduction

Active Galactic Nuclei (AGN) is a type of many celestial bodies, and it is an important research field in astrophysics in recent years [1]. Among them, the Blazar celestial body is an important part of the active galactic nucleus and represents a subclass of special observational properties. The ray-varying body has many characteristics that can reflect the nuclear nature of the active galaxies. It is a kind of active galactic nucleus with a small angle along the line of sight of the jet stream, and it is also a highly variable energy source with extremely high density. It has a series of unique physical properties such as radiation continuity, high luminosity, and strong radio and high polarization (optical polarization greater than 3%, radio polarization greater than 1% to 2%), which is the most obvious and intense light in all active galactic nuclei. Star. However, not all flare variants have exactly the same observational properties. According to the equivalent width of the emission line and the observed phenomena, the flare variants can be subdivided into two subclasses: flat-spectrum radio quasars (FSRQ) and scorpion tiger objects (BL Lac). Among them, the flat-spectrum radio quasars generally have a flat radio spectrum with a spectral index of less than 0.5 and an equivalent width of more than 5. However, the spectrum of Scorpion Tiger Object (BL Lac) is very weak or not, and its equivalent width is less than 5. The multi-band energy spectrum distribution (SED) of the flare variant has obvious bimodal structure. According to the position of its peak frequency of low-energy synchrotron radiation, the flare variant can be divided into three categories: low-synchrotron radiation peak flare variant (LSP, $<10^{14}$ Hz). Peak flare variants of moderate synchrotron radiation (ISP, $10^{14} < \nu_{\text{Speaks}} < 10^{15}$ Hz) and high synchrotron radiation (HSP, $\nu_{\text{Speaks}} > 10^{15}$ Hz). Scorpion-tiger celestial bodies can be divided into low peak frequency Scorpion-tiger celestial bodies (LBL) and high peak frequency Scorpion-tiger celestial bodies (HBL) according to their positions in SED. Generally speaking, the peak frequency of synchrotron radiation of LBLs is in the optical and infrared bands, while that of HBLs is in the ultraviolet-X-ray bands. Therefore, LSP generally includes flat-spectrum radio quasars and low peak frequency scorpion tiger objects (LBL) [2].

As a subclass of flare variants, flat-spectrum radio quasars have similar observation characteristics to Scorpion-Tiger objects. Generally speaking, there is strong broad emission line radiation in the spectrum of flat-spectrum radio quasars. The spectrum is non-thermal radiation and there is obvious photovariation. Radio wave band shows large photometric dispersion, large red shift, fast light change, high polarization, radio structure dominated by compact radio nuclei, high polarization and high light change. The results show that flat-spectrum radio quasars have strong correlations among compact radio radiation, high polarization and high light variability. The radiation of celestial bodies with these characteristics is non-thermal and relativistic. Moreover, the accretion rate of the flat-spectrum radio quasars is higher, and the external photon field is stronger.

The gamma-ray radiation of the flat-spectrum radio quasars may be generated by the external Compton scattering process. In addition, the optically dramatic quasar (OVV) is very similar to the scorpion corpus, with strong light changes and a high degree of linear polarization. However, OVV has a relatively wide transmission line. As the accuracy of the observations increased, almost all of the flat-spectrum radio quasars detected linear polarization, and later high-polarization quasars (HPQ) were discovered. Therefore, OVV and HPQ essentially classify them as flat-spectrum radio quasars. According to the position classification according to the peak frequency of the synchrotron radiation as described above, the flat spectrum radio quasar belongs to the LSP subclass [3, 4].

This paper focuses on the long-term timescales of flat-spectrum radio quasars. Section 2 introduces the SMARTS project, section 3 introduces a typical sample, the light change and color change of PKS 2142-75. Section 4 gives the statistical analysis of the sample, and section 5 summarizes it.

2. Data reduction

The observations used in this article are from the SMARTS (Small and Moderate Aperture Research Telescope System), Small and Medium Caliber Telescope System project (<http://www.astro.yale.edu/smarts/glast/home.php>)[5]. The project conducts approximately 700 hours of tracking observations per year on the Fermi satellite large-area telescope (Fermi-LAT) observation source observable in Chile. The small and medium-caliber telescopes used in the SMARTS project are located at the Intercontinental Observatory of the Torolo Mountains in northern Chile.

SMARTS 1.3m telescope and ANDCAM equipment are used in the routine monitoring program of SMARTS. ANDICAM equipment can provide dual-channel imaging for both infrared imaging equipment and optical CCD. Therefore, the simultaneous observation data of 0.4 to 2.2 microns can be obtained by this instrument. We can also measure the astronomical equivalence of objects in the field of view under extreme weather conditions. The optical counterparts of galaxy X-ray binaries have been observed in the monitoring activities of the SMARTS project for many years, and the same mass of data has been obtained from observations of flare variants. The SMARTS project also observed the spectra of the flare variants. Current studies have shown that many of the flare variants do not have particularly obvious spectra, but some show emission lines (e.g. 3C 273, PKS 1510-089), and can see changes in the intensity of emission lines. In addition, it is also possible that flares with no apparent lines appear in some special states. Therefore, when we observe the spectrum of the study, we select the spectra of the bright source of the rayon to study. The SMARTS 1.5m telescope only allows a spectral observation plan to be performed on a given night, so daily monitoring cannot be completed, and the spectrum of the target star can only be obtained every two to four weeks. The SMARTS project will publish and process the data as soon as possible, usually within 1-2 days of the LAT monitoring activity. The SMARTS project will continue to look for correlations between observational data and LAT data, and respond to interesting results and specific events to change observational strategies.

3. Light curve and color variability Of PKS 2142-75

3.1 Light Variation of PKS 2142-75

Figure 1 shows the historic B-band optical curve of the flat-spectrum radio quasar PKS 2142-75 from June 2010 to June 2015. In the figure, the abscissa is Julian day, the unit is sky, the ordinate is brightness, and the unit is magnitude. According to the chart, from 17.641 magnitude on June 11, 2010, after 459 days, it reached its darkest level on September 13, 2011, when the magnitude was 17.914 magnitude. After 1151 days, it reached its brightest on November 7, 2014, when the magnitude was 16.585. The eruption lasted 1610 days, and the magnitude of light variation reached 1.329 magnitude, with an average of 17.662 and a standard deviation of 0.183. Therefore, it can be seen that the activities of PKS 2142-75 are more intense.

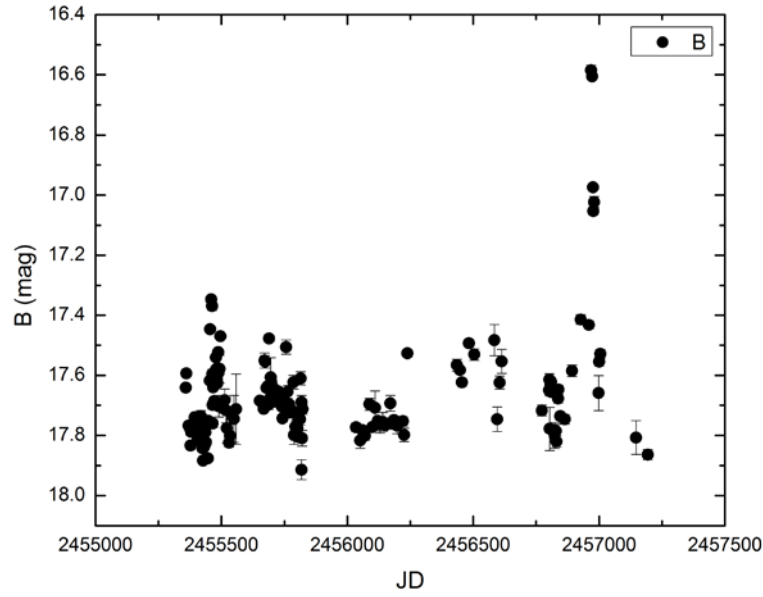


Fig.1.Optical B-band Historic Photodynamic Curves of Flat-spectrum Radio Star PKS 2142-75

Table 1 shows the statistics of the four bands of PKS 2142-75. Table 1 shows that the V-band of PKS 2142-75 has 165 data points, the maximum star equivalent value is 17.364 stars, the celestial body is the darkest, and the smallest star is 15.993 stars. The celestial body is the brightest, the brightest celestial body and the darkest celestial body. The star equivalents differ by 1.371 stars. Its average star value is 17.109 stars and the standard deviation is 0.198. The rest of the data is shown in Table 1. It can also be seen from Table 1. As the band frequency decreases (V to K band), the variation range of PKS 2142-75 becomes larger, and the average star increases. This is a flat spectrum radio class. The commonality of the stars.

Table 1 4 band data statistics Table of PKS 2142-75

Band	Observation data point (a)	Maximum (Magnitude)	Minimum value (Magnitude)	Variety (Magnitude)	average value (Magnitude)	standard deviation
V	165	17.364	15.993	1.371	17.109	0.198
R	202	17.026	15.486	1.54	16.654	0.219
J	205	16.341	13.77	2.571	15.298	0.532
K	226	15.249	11.839	3.41	13.524	0.660

3.2 Color change of PKS 2142-75

The so-called color index refers to the difference of stars in any two bands of the same celestial body. Its change is often a problem that researchers pay more attention to. Below we briefly analyze the color index of PKS 2142-75. We use the B-band and V-band observation data to obtain a color index of PKS 2142-75, with Julian day as the abscissa (unit: day) and color index (B - V) as the ordinate (unit: Star, etc.) plotted the color index curve of PKS2 142-75, as shown in Figure 2. The color change of the star is closely related to the size of the color index. In general, the greater the brightness of the star, the smaller the color index, and the closer the color of the star is to blue, this is the bluer-when-brighter (BWB) phenomenon [6, 7]. The greater the brightness of the star, the larger the color index, and the closer the color of the star is to red, this is the reder-when-brighter (RWB) phenomenon. The smaller the B-V color index during a short-term outbreak, the closer the color of the star will be to blue. If the color index is larger, the color of the star will be close to red. From June 11, 2010 to May 8, 2011, the color index decreased from 0.624 magnitude to 0.298 magnitude, reaching a minimum value. The change of color index is $_{(B-Va)} = 0.326$ magnitude. In a short period of more than three months, the color index of PKS 2142-75 reached its maximum on August 15, 2011, when it was 0.751 magnitude, and this change was also the fastest and most

drastic in the whole observation process. Subsequently, the color index began to decrease, its average value was 0.547, the standard deviation was 0.0796. When we carefully observe the color index curve, we can find that the color index of PKS 2142-75 is in a rapid decline, rapid rise, and the change is very intense. This may be due to the strong correlation between the bands, which also shows that the radiation mechanism of each band is the same.

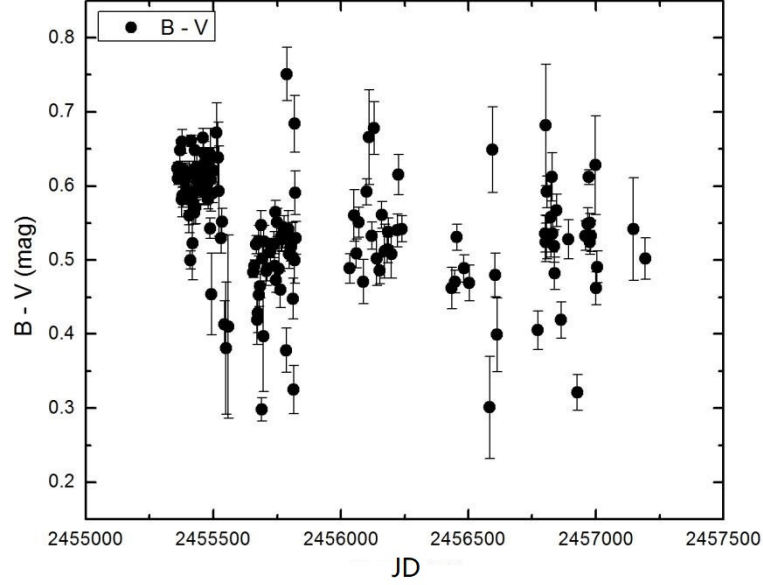


Fig.2. Change curve of color index of PKS2142-75

In order to further understand the photodynamic characteristics of the flat-spectrum radio quasar PKS 2142-75, we analyzed the correlation between flow and color index changes in B, V and (B+V)/2 bands as shown in Figure 3. The abscissa is B (unit: star, etc.), and the ordinate is the color index BV (unit: star, etc.) where the linear regression equation is $BV = (0.391 \pm 0.452) + (0.011 \pm 0.026) B$, and its slope is $a = 0.011 \pm 0.026$, the intercept is $b = 0.391 \pm 0.452$, the correlation coefficient is $r = 0.033$, and the confidence probability is $p = 0.682$. This shows that there is no correlation between B-band and color index changes.

When the abscissa is V (unit: star, etc.), the ordinate is the color index BV (unit: star, etc.) where the linear regression equation is $BV = (2.027 \pm 0.404) + (-0.085 \pm 0.024) V$, and its slope is $a = -0.085 \pm 0.024$, the intercept is $b = 2.027 \pm 0.404$, the correlation coefficient is $r = -0.277$, and the confidence probability is $p = 4.50195E-4$. It can be seen that there is a negative correlation between V band and color index.

When the abscissa is (B+V)/2 (unit: magnitude) and the ordinate is the color index B-V (unit: magnitude), the linear regression equation is $B-V = (1.272 \pm 0.438) + (-0.04 \pm 0.025) (B+V)/2$. Its slope is $a = -0.04 \pm 0.025$, the intercept is $b = 1.272 \pm 0.438$, the correlation coefficient $r = -0.126$, and the confidence probability is $p = 0.114$. It can be seen that the correlation between (BandV)/2 band and the change of color index is very poor.

The above analysis shows that PKS 2142-75 may exhibit the color change characteristics of RWB in the long-term range, but this change characteristic is not very strong.

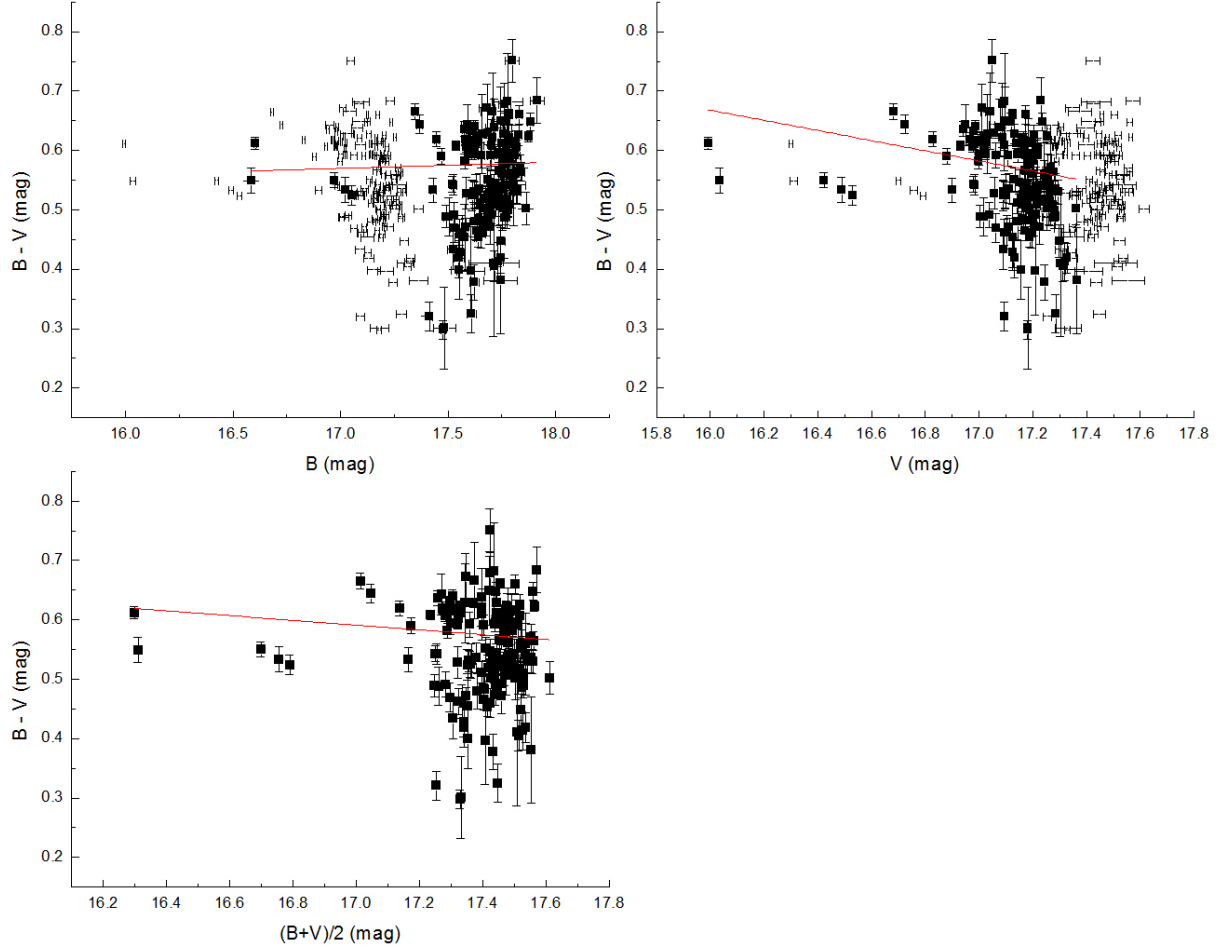


Fig.3. Linear regression analysis of brightness change and color index change of PKS 2142-75

4. Statistical Analysis of SMARTS Samples

In this paper, the same method is used to analyze the flat-spectrum radio quasar in the SMARTS sample. First, the color index $B-V$ is obtained, and then the correlation between the color index $B-V$ and $(B+V)/2$ is calculated. The specific results are shown in Table 2. In the Table, the first column is the target name, the second column is the average value of the color index BV , and the third column is the analysis result of the correlation between the color index BV and $(B+V)/2$, followed by the slope, correlation Coefficient, confidence probability, and color characteristics. In this paper, the correlation coefficient is greater than 0.2 and the confidence probability is less than 0.01, which indicates that there is a significant positive correlation between the color index and the flow, that is, there is a BWB color characteristic between the two. When the correlation coefficient is less than 0.2 and the confidence probability is less than 0.01, it shows that there is a significant negative correlation between the color index and the flow, that is, there is a RWB color characteristic between the two. In addition, it shows that there is no correlation between them, expressed by NONE.

From the above analysis of the color index mean, slope, correlation coefficient and confidence probability parameters, it can be seen that the correlation between the brightness change of the flat-spectrum radio quasar and the color index change is negatively correlated in some cases. In some cases, there is a positive correlation, while in other cases, there is no correlation. Such a situation may result in no color change in the case of long time scales, which reflects the complexity of light changes of different targets. At the same time, the increase and decrease of the flow rate may be accompanied by different color changes, and also reflect the difference in the time when the flow rate of each band reaches the peak value. The specific color analysis showed that among the 23 targets, 2 showed BWB, accounting for 8.696%, 3 showed RWB characteristics, accounting for

13.043%, and 18 did not show color change characteristics, accounting for 78.261%.

Table 2 Analysis of the correlation between flat-spectrum radio quasars B-V and (B+V)/2 in SMARTS samples

Target name	Mean value of color index	Slope	Correlation coefficient	Confidence probability	Color characteristics
0017-0512	-2.958	-0.171±0.032	-0.738	1.662E-5	RWB
0250-225	0.632	-0.701±0.136	-0.601	4.908E-6	RWB
0402-362	0.228	-0.053±0.02	-0.253	0.012	NONE
0454-46	0.428	-0.11±0.188	-0.103	0.563	NONE
0454-234	0.564	0.042±0.007	0.308	1.023	NONE
0502+049	0.619	-0.022±0.047	-0.086	0.640	NONE
0637-75	0.242	2.088±0.163	0.908	9.437	NONE
0850-1213	0.415	0.138±0.078	0.297	0.088	NONE
1004-217	0.189	0.913±0.245	0.550	7.560	NONE
1144-379	0.583	0.137±0.032	0.337	2.746E-5	BWB
3C 273	0.232	0.553±0.0478	0.548	0	BWB
3C 279	0.527	0.0147±0.007	0.079	0.047	NONE
1406-076	0.384	-0.098±0.0171	-0.401	4.551	NONE
1510-089	0.327	-0.107±0.006	-0.586	0	RWB
1550-242	0.707	0.042±0.045	0.0472	0.422	NONE
1622-297	0.686	-0.07±0.02	-0.227	5.147	NONE
1730-130	0.965	0.003±0.023	0.008	0.905	NONE
1954-388	0.447	-0.269±0.168	-0.47	0.144	NONE
2052-474	0.344	-0.053±0.007	-0.5	9.870	NONE
3c 446	3.356	-0.186±0.168	-0.363	0.302	NONE
3c 454.3	0.567	-0.006±0.005	-0.046	0.212	NONE
2255-282	0.520	-0.035±0.225	-0.048	0.881	NONE
2345-16	0.451	0.017±0.02	0.153	0.420	NONE

5. Conclusion

The light change and color change of celestial bodies are important observational features of the flat-spectrum radio quasars, and their research and analysis can deepen our understanding and understanding of their energy mechanisms and peripheral environment. The flat-spectrum radio quasar PKS 2142-75 is very active and has good observations throughout the band. We obtained the historic photodynamic curves and color index curves of the optical B, V, R, J and K bands of PKS 2142-75 from August 2008 to March 2015, and analyzed their correlation and color.

The photodynamic curves of PKS 2142-75 show that the photodynamic activities of celestial bodies are very intense in each band, and explosive phenomena often occur. In addition, when we carefully observe the change curve of the color index, we can find that the color index of PKS 2142-75 is in a rapid decline and rise, and the change is very intense. This may be due to the correlation between the bands, which indicates that the optical variability of each band has a common physical origin, and the radiation generation of each band may be based on the same physical mechanism. In addition, we use the linear regression method to linearly fit the color index and each band (B, V, (B+V)/2). It is shown that the correlation between the bands can be found from the color index curve. Not very strong. The analysis of the relationship between the change of brightness under the long time scale and the color change of the color index shows that the long time scale range is monochromatic, which reflects the complexity of different target light changes, and also shows the PKS 2142- 75 light changes are very complicated. Finally, the objectives of all the flat-spectrum radio quasars in the SMARTS source are analyzed and organized in tabular form. The results show that in the flat-spectrum radio quasars, some of the correlations between the

change of brightness and the change of color index are negatively correlated, some are positively correlated, and most of them show no correlation.

References

- [1] Clark T D, Sandblom E, Jutfelt F. Aerobic scope measurements of fishes in an era of climate change: respirometry, relevance and recommendations [J]. *Journal of Experimental Biology*, 2013, 216(15):2771-2782.
- [2] Tang X, Holland D, Dale A M, et al. The diffeomorphometry of regional shape change rates and its relevance to cognitive deterioration in mild cognitive impairment and Alzheimer's disease [J]. *Human Brain Mapping*, 2015, 36(6):2093-2117.
- [3] Liu H, Pu S, Liu G, et al. Photochromism of asymmetrical diarylethenes with a pyrimidine unit: Synthesis and substituent effects [J]. *Dyes and Pigments*, 2014, 102:159-168.
- [4] Gong X, Jin Y Q. Diurnal change of MW and IR thermal emissions from lunar craters with relevance to rock abundance[J]. *Acta Astronautica*, 2013, 86(Complete):237-246.
- [5] Cinquini L, Collini P, Marelli A, et al. Change in the relevance of cost information and costing systems: evidence from two Italian surveys [J]. *Journal of Management & Governance*, 2015, 19(3):557-587.
- [6] Kim H, Grunkemeyer T J, Modi C, et al. Acid–Base Catalysis and Crystal Structures of a Least Evolved Ancestral GFP-like Protein Undergoing Green-to-Red Photoconversion[J]. *Biochemistry*, 2013, 52(45):8048-8059.
- [7] Juraj Bujdák. Hybrid systems based on organic dyes and clay minerals: Fundamentals and potential applications [J]. *Clay Minerals*, 2015, 50(5):549-571.